THE JOURNAL OF BIOLOGICAL CHEMISTRY VOL. 286, NO. 34, pp. 29725–29733, August 26, 2011

Pulmonary Biocompatibility Assessment of Inhaled Single-wall and Multiwall Carbon Nanotubes in BALB/c Mice*

Received for publication, April 15, 2011, and in revised form, June 16, 2011 Published, JBC Papers in Press, June 24, 2011, DOI 10.1074/jbc.M111.251884

Prabakaran Ravichandran[‡], Sudhakar Baluchamy[§], Ramya Gopikrishnan[‡], Santhoshkumar Biradar[‡], Vani Ramesh[‡], Virupaxi Goornavar[‡], Renard Thomas[¶], Bobby L. Wilson[¶], Robert Jeffers[‡], Joseph C. Hall[‡], and Govindarajan T. Ramesh[‡1]

From the [‡]Molecular Toxicology Laboratory, Center for Biotechnology and Biomedical Sciences, Department of Biology, Norfolk State University, Norfolk, Virginia 23504, the [§]Department of Biotechnology, Pondicherry University, Pondicherry 605014, India, and the [¶]Department of Chemistry, Texas Southern University, Houston, Texas 77004

With the widespread application of carbon nanotubes (CNTs) in diverse commercial processes, scientists are now concerned about the potential health risk of occupational exposures. In this study, CNT-induced pulmonary toxicity was investigated by exposing BALB/c mice to aerosolized single-wall (SW) CNT and multiwall (MW) CNT (5 μg/g of mice) for 7 consecutive days in a nose-only exposure system. Microscopic studies showed that inhaled CNTs were homogeneously distributed in the mouse lung. The total number of bronchoalveolar lavage polymorphonuclear leukocytes recovered from the mice exposed to SWCNT and MWCNT ($1.2 \times 10^6 \pm 0.52$ and $9.87 \times 10^5 \pm 1.45$; respectively) was significantly greater than control mice ($5.46 \times 10^5 \pm 0.78$). Rapid development of pulmonary fibrosis in mice that inhaled CNT was also confirmed by significant increases in the collagen level. The lactate dehydrogenase levels were increased nearly 2- and 2.4-fold in mice that inhaled SWCNT and MWCNT, respectively, as compared with control mice. In addition, exposure of CNTs to mice showed a significant ($p < 0.05$) reduction of antioxidants (glutathione, superoxide dismutase, and catalase) and induction of oxidants (myloperoxidase, oxidative stress, and lipid peroxidation) compared with control. Apoptosis-related proteins such as caspase-3 and -8 activities were also significantly increased in mice that inhaled CNT than in control mice. Together, this study shows that inhaled CNTs induce inflammation, fibrosis, alteration of oxidant and antioxidant levels, and induction of apoptosis-related proteins in the lung tissues to trigger cell death.

Carbon nanotubes (CNTs)[2] are regarded as a novel material, because of their unique physicochemical properties, and we find its application in various fields (1). Because of the fibrous shape, extreme aspect ratio, low specific density, and low solubility, CNTs might exhibit toxicity similar to that of asbestos (2). Although CNTs come in a variety of types, single-wall carbon nanotubes (SWCNT) and multiwall carbon nanotubes (MWCNT) are currently the predominant forms being studied. Because of their increased use in commercial applications, the potential health effects of CNTs following inhalation are of great interest particularly pulmonary exposure in the work place.

Three major factors such as the shape of the particle, the surface reactivity, and its clearance from the respiratory tract determine the biocompatibility of the inhaled particles (3). From such criteria, CNTs appear as potentially highly harmful particles. The effects of nanoparticle exposure seen in *in vitro* studies indicate a role of oxidative stress in the production of inflammatory cytokines and cytotoxic responses (4, 5). Other consequences of oxidative injury include effects on nuclear factor activation, gene transcription, and protein expression (6, 7).

Virtually all the *in vivo* studies have utilized nonphysiological routes of pulmonary exposure like intratracheal instillation or nasopharyngeal aspiration in rodents, which results in lung injury (8). The first study with SWCNT reported no significant signs of lung toxicity 4 weeks after intratracheal administration in guinea pigs (9). Conversely, acute lung toxicity of intratracheally instilled SWCNT has been evaluated in rats, and it has been reported that exposure to SWCNT produced transient inflammation and a nondose-dependent formation of multifocal granulomas (10). The toxicological significance of these granulomas was questioned because their formation was possibly due to the instillation of a bolus of agglomerated SWCNT. A previously published report (11) on the mouse model showed that exposure of SWCNT by pharyngeal aspiration caused transient dose-dependent inflammation. After exposure, both compact aggregates and dispersed structures were observed in the lung (11).

Concerning MWCNT, Muller *et al.* (12) investigated the effects of intact or milled MWCNT by intratracheal instillation to female Sprague-Dawley rats and observed a dose-dependent and persistent inflammation and granuloma formation. These studies show that CNTs, which aggregate into micron-sized bundles in aqueous media, stimulate the formation of inflammatory foci known as granulomas and fibrotic reactions within the lung parenchyma. The existing information on pulmonary toxicity of CNTs is very limited, and existing results are also not consistent. Therefore, increased emphasis has been placed on

* This work was supported, in whole or in part, by National Institutes of Health Grant 1P20MD001822-1. This work was also supported by NASA Grants NNX08BA47A, NCC-1-02038, NSTI, and NSF CREST.

[1] To whom correspondence should be addressed. Tel.: 757-823-8951; Fax: 757-823-2618; E-mail: gtramesh@nsu.edu.

[2] The abbreviations used are: CNT, carbon nanotube; SWCNT, single-wall carbon nanotube; MWCNT, multiwall carbon nanotube; TEM, transmission electron microscope; BAL, bronchoalveolar lavage; BALF, bronchoalveolar lavage fluid; LDH, lactate dehydrogenase; ROS, reactive oxygen species; LPO, lipid peroxidation; SOD, superoxide dismutase; AFC, 7-amino-4-trifluoromethylcoumarin; MPO, myeloperoxidase; PMN, polymorphonuclear leukocyte.

determining the most relevant method to study the biocompatibility of CNTs than injection because materials completely bypass the lung and its defense and clearance mechanisms entirely. These features led us to develop an inhalation protocol to investigate the pulmonary toxicity of occupationally relevant single and multiwall carbon nanotube exposure using male BALB/c mice. To check the pulmonary toxicity, the cytotoxic potential was estimated by determining LDH and total protein contents in bronchoalveolar lavage fluid (BALF). The basic molecular mechanism exhibited by CNTs was elucidated by examining the antioxidant levels and apoptotic signaling pathway that involve caspase-8 as well as caspase-3.

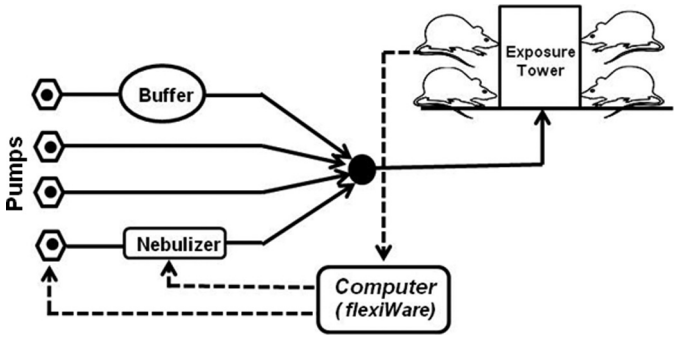

FIGURE 1. **Schematic layout of the nose-only exposure experimental setup for CNT exposure in mice (inExpose, Scireq, Canada).** The inExpose is fully computer-controlled using the software flexiWare.

EXPERIMENTAL PROCEDURES

Animals and Experimental Design—Male BALB/c mice (Hilltop Lab Animals, Inc., Scottdale, PA), 2–3 weeks of age and weighing 20 ± 2 g, were kept under conventional housing conditions (24–26 °C, with 55–75% humidity, and a 12-h light/dark cycle). Mice were maintained on special dietary food (Hilltop Lab Animals, Inc.) and given tap water *ad libitum*. The acclimatization period was 7 days before use. At the end of the acclimatization period, mice were randomized by weight and divided into three experimental groups as follows: control, SWCNT, and MWCNT (six mice per group). Mice were exposed to aerosolized CNTs for 20 min/day (5 μg/g of mice) or phosphate-buffered saline (PBS, vehicle) for 7 consecutive days in a nose-only exposure system (In Expose, Scireq, Canada), and returned to the vivarium. After 7 days of exposure, the animals were sacrificed; lung tissues were collected and stored at −80 °C until analyzed.

Animal Exposure—For aerosol, the mixture was prepared by suspending the autoclaved CNTs (SWCNT and MWCNT) in sterile biocompatible nonionic surfactant, 1% Tween 20 (Bio-Rad) by sonication for 5 min using 50% amplitude and oscillating cycles and pause of 30 s each (Qsonica, LLC) to form a CNT suspension (0.5 mg/ml). The control vehicle group receive sterile PBS (pH 7.4) (Atlanta Biologicals, Inc., Atlanta, GA) containing sterile, 1 weight % Tween 20. The other experimental groups received SWCNT and MWCNT suspended in sterile PBS containing 1% Tween 20. Nebulizer (Aeroneb Scireq, Montreal, Canada) was used to aerosolize the nanotubes at a constant rate of 0.005 ml/min and diluted with compressed room air using an external pump at a flow rate of 3 liters/min. The nebulizer was connected to the top part of the central tower from which the generated aerosol flowed down to the peripherally arranged mice (six mice). Each mouse was held in a soft restrainer such that only the nose was exposed to the aerosol cloud (Fig. 1).

Lung Histopathology—Lungs from control and exposed mice group were fixed with 10% neutral buffered formalin and processed using routine histological techniques. Briefly, after paraffin embedding, 5-μm sections were cut and stained with hematoxylin and eosin (H&E) for histopathological evaluation.

Electron Microscopy—Lungs were collected from the control and exposed group mice and fixed in McDowell's and Trump's 4F:1G fixative with negative pressure. The lung tissues were then post-fixed in 0.1 M sodium phosphate buffer (pH 7.2), containing 1% osmium tetroxide, dehydrated through graded ethanol solutions, cleared in acetone, infiltrated, and embedded in Spurr's resin. Unstained thin sections were mounted on copper grids and then examined on a Philips EM208S transmission electron microscope (TEM).

Bronchoalveolar Lavage—The right lung lobes were serially lavaged three times with 2.0 ml of sterile cold PBS, after ligating of the left bronchus. BALF collected from each individual mouse were washed in PBS by alternate centrifugation (800 × g, 10 min, 4 °C), and the pellets were resuspended in PBS containing 2% FBS. Cytospinning was performed with 500 μl of BAL fluid harvested at the selected time intervals. After cytospinning, slides were fixed in methanol and stained with modified Wright-Giemsa stain, and cell differentials were determined by light microscope. Total cell numbers and different cell types in the BAL fluid were quantified by their characteristic morphologies (13).

BAL Fluid Lactate Dehydrogenase Assay and Total Measurements—The left lobes were lavaged once with 2 ml of PBS. The obtained BALF was centrifuged (800 × *g*, 10 min) at about 4 °C. Using an aliquot of the lavage supernatant, the activity of lactate dehydrogenase (LDH) was assayed spectrophotometrically by monitoring the reduction of nicotinamide adenine dinucleotide at 340 nm in the presence of lactate. This was performed using lactate dehydrogenase reagent set (LD Liquid Reagent; Pointe Scientific, Canton, MI), and total protein in the BAL fluid was estimated by a modified Bradford assay according to the manufacturer's instructions (Coomassie Plus Protein Assay Reagent; Pierce), and the remainder was frozen at −80 °C until processed.

Collagen Assay—Fibrosis was assessed by quantifying total soluble collagen using the Sircol collagen assay kit (Biocolor Ltd., Carrickfergus, UK). Briefly, lungs were wet weighed and homogenized in 0.7 ml of 0.5 M acetic acid containing pepsin with a 1:10 ratio of pepsin tissue to wet weight. Each sample was stirred vigorously for 24 h at 4 °C and centrifuged, and 200 μl of supernatant was assayed for soluble collagen according to the manufacturer's instructions. Absorbance at 540 nm was read on a FLUOstar Omega (BMG Labtech). Data were expressed as milligrams of soluble collagen per mg of total proteins.

Preparations of Lung Homogenate—At the end of the 7 days of CNT exposure, whole lung tissues were excised under anesthesia. The lung tissues were washed thoroughly in ice-cold PBS and weighed. A 10% homogenate of each tissue was pre-

pared separately in 10 mM Tris buffer (pH 7.4) containing protease inhibitor mixture, using a motor driven Teflon pestle homogenizer (Sigma), followed by sonication (Branson Sonifier, Fisher) and centrifugation at 500 × *g* for 10 min at 4 °C. The supernatant was aspirated and centrifuged again at 2000 × *g* for 60 min at 4 °C. The supernatant obtained after centrifugation was called "tissue lysate" and was used for the assays.

Oxidative Stress Assay—The intracellular reactive oxygen species (ROS) were measured as described earlier (14). ROS production was quantified by the 2,7-dichlorodihydrofluorescein method. 2′,7′-Dichlorofluorescein diacetate reacts with ROS to form the highly fluorescent compound dichlorofluorescein. Briefly, 50 μg of protein from each tissue lysate was mixed with 10 μl of 2′,7′-dichlorofluorescein (10 μM). Fluorescence of the samples was monitored at an excitation wavelength of 485 nm and an emission wavelength of 538 nm using fluorescence plate reader (FLUOstar Omega (BMG Labtech).

Lipid Peroxidation Assay—The extent of lipid peroxidation (LPO) in control and CNT-exposed mouse lungs was determined by measuring malondialdehyde, which is a thiobarbituric acid-reactive substance. Malondialdehyde levels were determined according to the procedure described earlier (15). Briefly, 50 μg of proteins were extracted from each tissue lysate using chloroform followed by mixing with chloroform/methanol, and freshly prepared chromogen was added, and absorbance was measured at 500 nm.

Myeloperoxidase Assays—To determine whether inhalation of CNTs causes the release of myeloperoxidase (MPO) into lavage fluids, the assay was performed as described earlier (16). 100 μl of fresh bronchoalveolar lavage supernatant containing 15 μg of protein was mixed with 100 μl of fresh 3,3′-5,5′-tetramethylbenzidine reagent prepared from a stock solution of 300 mmol/liter sodium acetate buffer (pH 5.4), 15 mmol/liter tetramethylbenzidine prepared in dimethylformamide, and 60 mmol/liter H_2O_2. The oxidation of tetramethylbenzidine by myeloperoxidase was measured at 630 nm over a 20-min period, with readings at every 5 min.

Total SOD Assay—The activity of SOD was measured as described earlier (17). Briefly, 50 μg of protein from tissue lysates were incubated with xanthine oxidase enzyme and tetrazolium salt for 20 min at 37 °C. Finally, xanthine oxidase solution was added to each sample, and the absorbance of the formazan salt resulting from the oxidation of tetrazolium salt was detected at 550 nm. The activity of SOD, expressed as percent inhibition of the formation of formazan, was then calculated by using an equation provided in the manufacturer's instructions (catalog no. 7500-100k, R&D Systems, Inc.).

Catalase Assay—The activity of catalase enzyme was measured as described previously (18). An appropriate volume of tissue lysate containing 50 μg of protein from each sample was mixed with 1 ml of 50 mM potassium phosphate buffer (pH 7.0) containing 10 mM H_2O_2 in a 1-ml quartz cuvette. The decrease in absorbance of H_2O_2 was followed at 240 nm for 5 min. Catalase activity was calculated from the slope of the H_2O_2 absorbance curve and normalized to protein concentration.

Glutathione Assay—The activity of glutathione (GSH) was directly measured as described earlier (5). Briefly, 50 μg of protein from tissue lysate from each sample was diluted to 1:2 ratios with 5% 5-sulfosalicylic acid dihydrate solution and sodium carbonate (400 mM) followed by 1:8 dilutions with phosphate/EDTA buffer and incubated for 10 min at room temperature. Ten microliters of 5–5′-dithiobis-2-nitrobenzoic acid substrate solution was added to each sample tube and incubated again at room temperature for 10 min. The GSH activity was measured at 415 nm absorbance.

TABLE 1
The physiochemical properties of single wall and multiwall carbon nanotubes used in this study

	SWCNT	MWCNT
Provider	Aldrich	Sigma
Product number	652512	698849
Diameter (nm)	1-2	20-50
Wall thickness	0.8-1.6	1-2
Length	0.5-2.0 μm	6-13 nm
Purity	>90%	>99%
Production method	CCVD	CCVD
Catalyst	Fe	Ni

Caspases Assay—Caspase-3 and -8 activities were measured in the control and CNT-exposed lung homogenate, as described previously (17). Cleavage activities of caspase-3 and -8 substrates DEVD-AFC and IETD-AFC were measured. Briefly, 50 μg of protein extracts from each tissue lysate were mixed with DEVD-AFC and IETD-AFC substrates and incubated for 1 h at 37 °C for detecting caspase-3 and -8, respectively. The formation of free AFC in the extract was measured at an excitation wavelength of 400 nm and an emission wavelength of 495 nm. The values of experimental samples were compared with control and expressed as fluorescence units.

Western Blotting—Samples containing 100 μg of cellular protein were subjected to standard Western blot analysis (6, 7). Briefly, proteins were separated using 10% SDS-polyacrylamide gel and transferred to a polyvinylidene difluoride membrane. Immunoblotting was performed by blocking overnight with 5% nonfat milk in PBS, 0.1% Tween, probed with appropriate primary antibody followed by secondary antibody conjugated with horseradish peroxidase, and developed using chemiluminescence reagent (GE Healthcare).

Statistical Analysis—The results obtained from the CNT-exposed groups was compared with control group. The values were calculated using Student's *t* test, and levels of significance were represented for each result.

RESULTS

Carbon Nanoparticles Characterization—The physicochemical properties of SWCNT and MWCNT used in this study are showed in Table 1. Scanning electron micrographs determined

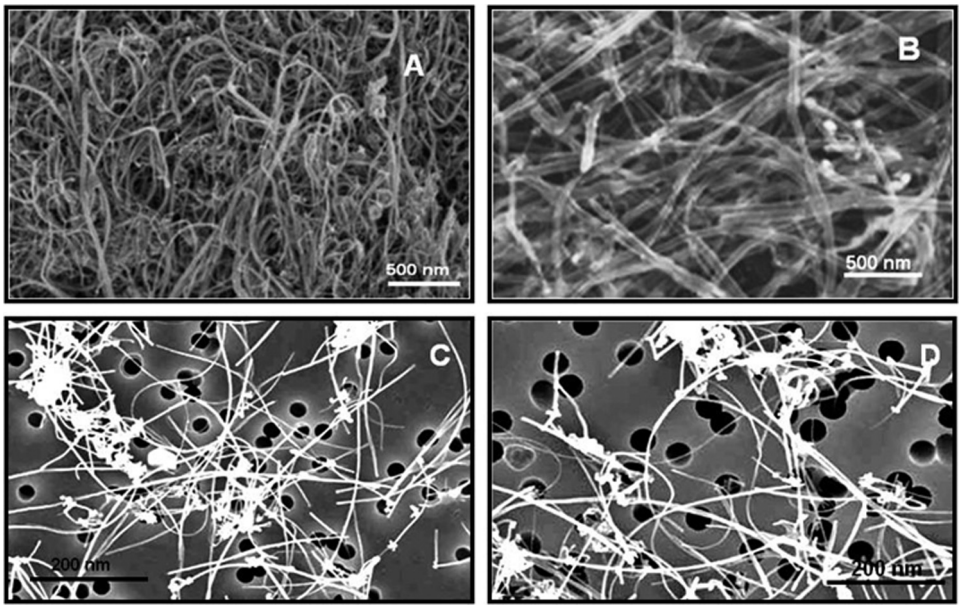

FIGURE 2. **Scanning electron micrographs of carbon nanotubes.** *A,* SWCNT; *B,* MWCNT. Field emission scanning electron microscopy of the carbon nanotubes dispersed in the PBS + 1% Tween 20 is shown. *C,* SWCNT. *D,* MWCNT. The micrograph was showing good dispersion after 5 min of ultrasonication.

that the nanotubes that we used here were SWCNT and MWCNT and not some other form of carbon nanoparticle or amorphous carbon (Fig. 2, *A* and *B*). Field emission scanning electron micrographs confirm that the autoclaved CNTs were well dispersed in sterile PBS + 1% Tween 20 solution (Fig. 2, *C* and *D*). Thus, any toxicological outcomes determined in this study can be attributed to exposure to SWCNT and MWCNT.

Estimation of CNT Aerosol Exposed to Mice—To identify the exact amount of CNTs exposed to the BALB/c mice, a gravimetric sampling method was employed as described previously (19). The weight of the nanotubes collected was determined by weight of the substrate (glass fiber filters; 0.7-μm pore size; Millipore) both before and after sampling. All filters were dried at 30 °C and weighed. Filters exposed to control vehicle group under the same experimental conditions were used as blanks. The average weight of SWCNT and MWCNT in the aerosol ($\pm$S.D.) was 93 $\pm$ 2 μg/ml, and this value did not vary significantly during exposures. Thus, every BALB/c mouse was exposed to CNTs approximately equivalent to 5 μg/g of mice; this is consistent with the CNT concentrations reported earlier, which showed an induction of oxidative stress and cytotoxicity under *in vitro* conditions (5, 14).

Histopathology of CNT-exposed Lung Tissue—No overt signs of stress and weight loss or gain were observed in both experimental and control groups during the study period. The histology of lung exposed to PBS + 1% Tween 20 is shown in Fig. 3*A*. The bright field microscope of lung sections showed that inhaled SWCNT and MWCNT were homogeneously distributed (Fig. 3, *B* and *C*). In particular, the distribution of SWCNT and MWCNT in lung tissues showed some agglomerates on the surfaces of alveolar ducts, indicating delivery of the aerosol to the distal airways (Fig. 3, *B* and *C*). Increased accumulation of polymorphonuclear leukocytes (PMNs) was observed in the lung section of exposed groups as compared with control groups (Fig. 3*D*). The presence of both SWCNT and MWCNT

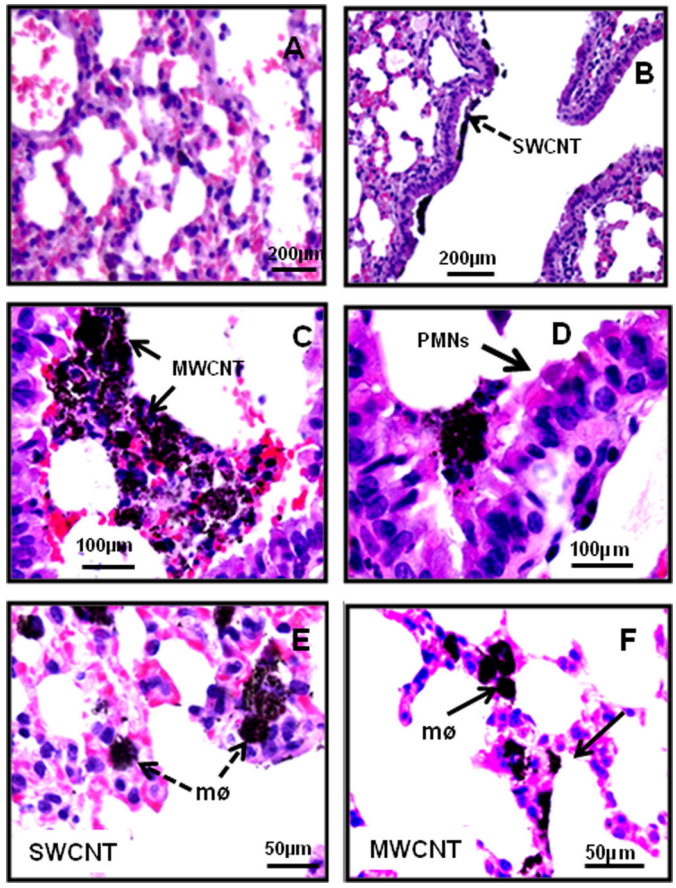

FIGURE 3. **Histopathology of lung tissues after 7 successive days of aerosol exposure of CNTs.** Lung sections are from mice exposed to control PBS + 1% Tween 20 (*A*), SWCNT (*B*), and MWCNT (*C*). The lung sections were stained with hematoxylin and eosin. *Dashed* and *solid arrows* point to SWCNT and MWCNT, respectively. *D,* inflammation, characterized by the accumulation of PMNs around CNTs. *E* and *F,* light microscopy of SWCNT (*dashed arrow*) and MWCNT (*solid arrow*) in macrophages (*mø*) after 7 successive days of inhalation of CNTs.

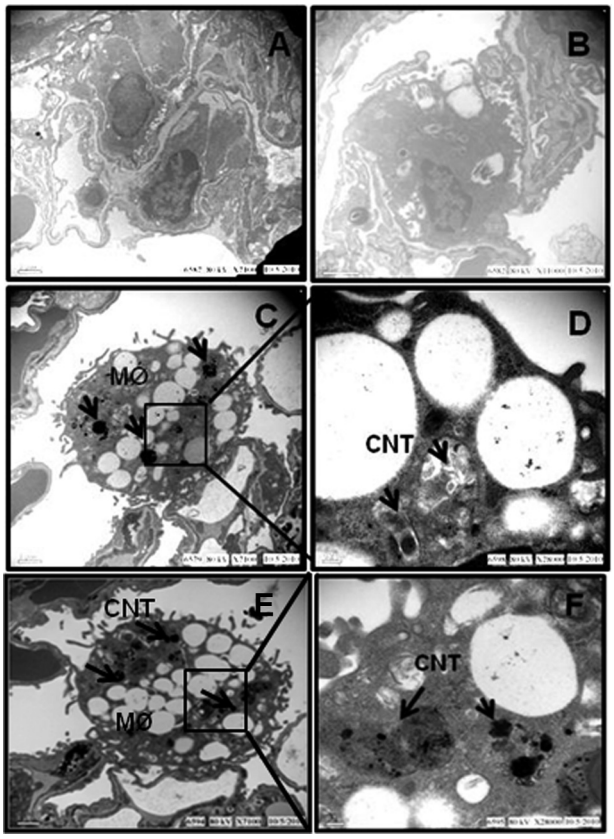

FIGURE 4. **TEM examination of CNT distributions in lung tissue.** *A* and *B*, TEM image of control group exposed to PBS + 1% Tween 20. *C* and *E*, TEM of SWCNT and MWCNT within an alveolar macrophage (*mø*). *D* and *F*, higher magnification of SWCNT and MWCNT showing nanotube within macrophages.

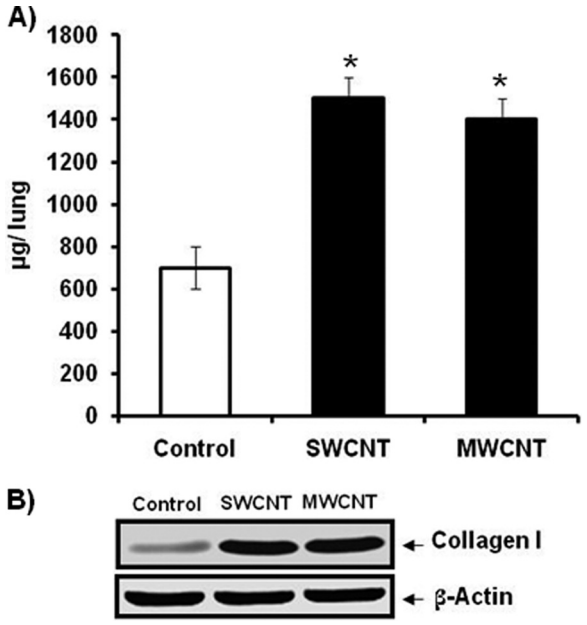

FIGURE 5. **Carbon nanotubes induce pulmonary fibrosis.** *A,* fibrosis was assessed by quantifying total soluble collagen using the Sircol collagen assay kit. The experimental values were compared with control and expressed as micrograms/lung. Values are means ± S.D. of three independent experiments. *, *p* value <0.05 was estimated by Student's *t* test. *B,* 50 µg of proteins were resolved on SDS-PAGE and assayed for collagen I using specific antibody. The blots were stripped off and reprobed with β-actin antibody for loading control.

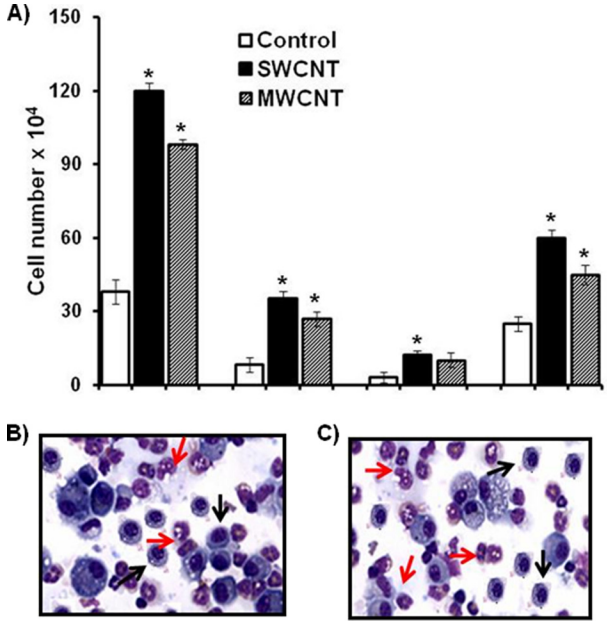

FIGURE 6. **Pulmonary inflammation induced by SWCNT and MWCNT.** Mice were exposed to aerosolized CNTs (5 µg/g of mouse) and PBS + 1% Tween 20 (vehicle). *A,* differential cell counts were performed on 500 cells to identify neutrophils, eosinophils, and macrophages. Results are means ± S.E. ($n = 6$ in each group). Values are means ± S.D. of three experiments performed independently. *, *p* value <0.05 was estimated by Student's *t* test. *B* and *C,* light micrographs of BAL cell cytospins obtained from SWCNT- (*B*) and MWCNT (*C*)-exposed mouse lungs stained using modified Wright-Giemsa stain. Both CNT exposures show the presence of numerous PMNs (*red arrow*) and macrophages (*black arrow*).

was observed in alveolar macrophages after 7 successive days of inhalation (Fig. 3, *E* and *F*). However, TEM identified small aggregates and individual CNTs within alveolar macrophages (Fig. 4, *C* and *E*). Some of the macrophages contain large masses of CNT fibers or agglomerates in the vacuolated areas (Fig. 4, *D* and *F*). The TEM of lung exposed to control vehicle group was shown in Fig. 4, *A* and *B*.

Carbon Nanotubes Induce Pulmonary Fibrosis—Next, we examined whether these inhaled nanotubes could induce lung fibrosis. Fig. 5*A* shows that both SWCNT and MWCNT were able to increase lung collagen content as compared with control. This is also confirmed by Western blot (Fig. 5*B*).

Carbon Nanotubes Induce Pulmonary Inflammation—Pulmonary inflammation was evaluated by determining the number of increasing BAL PMNs in the mice treated with SWCNT and MWCNT and the control group. The inhalation of both CNTs significantly increased the total number of cells in BAL fluid. The total number of cells recovered from the BALF of SWCNT and MWCNT exposed mice ($1.2 \times 10^6 \pm 0.52$ and $9.87 \times 10^5 \pm 1.45$; respectively) was significantly greater than control mice ($5.46 \times 10^5 \pm 0.78$) (Fig. 6*A*). With the increase in total cell numbers, the percent composition of neutrophils, eosinophils, and macrophages was significantly higher in both mice that inhaled CNT SWCNT and MWCNT compared with control mice (Fig. 6*A*). Wright-Giemsa staining of CNT exposed lungs show the presence of numerous PMNs and macrophages (Fig. 6, *B* and *C*).

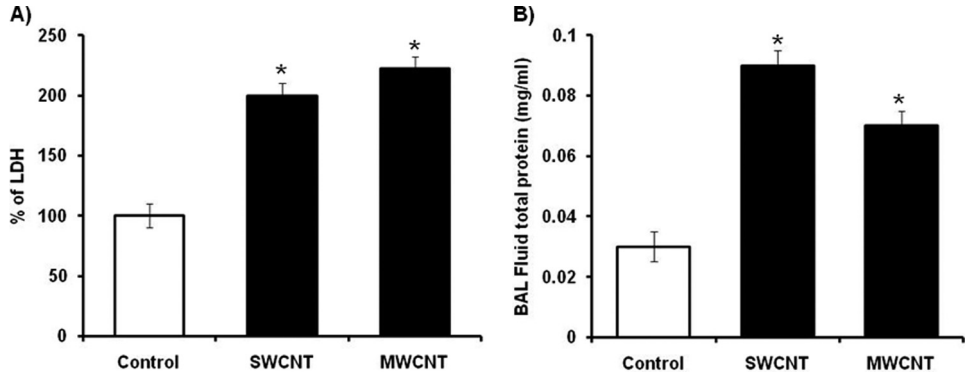

FIGURE 7. **Carbon nanotube exposure increases LDH levels in BAL fluid and total protein concentration.** Mice were exposed to aerosolized CNTs (5 μg/g of mouse) and PBS + 1% Tween 20 (vehicle). BAL fluid was obtained after 7 successive days of exposure. *A,* LDH level was assayed spectrophotometrically by monitoring the reduction of nicotinamide adenine dinucleotide at 340 nm in the presence of lactate as substrate. *B,* total protein in the BAL fluid was performed by a modified Bradford assay according to the manufacturer's instructions. Values are means ± S.D. of three experiments performed independently. *, p value <0.05 was estimated by Student's t test.

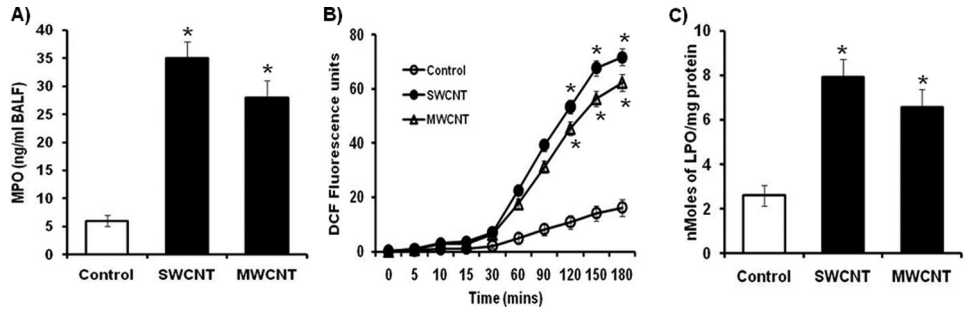

FIGURE 8. **Inhalation of carbon nanotubes activates MPO, ROS, and LPO in the BALF/lung homogenates.** BAL fluid was collected from mice that inhaled CNTs and lungs from control mice. *A,* levels of MPO in the BAL fluids were performed as described earlier. The oxidation of tetramethylbenzidine by myeloperoxidase was measured at 630 nm. After BAL, the lung homogenates were prepared from CNTs of exposed and control mouse lungs. *B,* 50 μg of total proteins from each tissue lysate was mixed with 10 μl of 2,7-dichlorodihydrofluorescein (10 μM). Fluorescence of the samples was monitored at an excitation wavelength of 485 nm and an emission wavelength of 538 nm. *C,* 50 μg of protein was used to measure the level of malondialdehyde in control and CNT-exposed mice at 500 nm to determine the lipid peroxidation. Values are means ± S.D. of three experiments performed independently. *, p value <0.05 was estimated by Student's t test.

Carbon Nanotubes Induce Cytotoxicity—BAL fluid LDH activity, a marker of cell toxicity, was significantly increased after CNTs inhalation as compared with control. The LDH levels were increased nearly by 2 and 2.4 times in mice that inhaled SWCNT and MWCNT, respectively, as compared with control mice (Fig. 7*A*). The protein concentration in BAL fluid, which reflects alveolocapillar permeability and/or alveolitis, was also increased after inhalation of CNTs (Fig. 7*B*). Together, we conclude that CNTs induce an inflammatory response in mice lungs.

Carbon Nanotubes Activate Oxidative Stress—To check whether inhaled CNTs induce oxidative stress in the lung, we first measured MPO, ROS, and LPO levels in the BALF/lung homogenates from exposed mice and controls (Fig. 8, *A–C*). MPO activity was higher in the BALF fluid prepared from both CNT exposed groups (SWCNT nearly 7-fold and MWCNT 5-fold) than the control group (Fig. 8*A*). As shown in Fig. 8*B*, both SWCNT and MWCNT activated ROS significantly as compared with control. ROS levels were higher with an ~4-fold in SWCNT and a 3.5-fold in MWCNT inhaled group than the control group (Fig. 8*B*). Because increased concentrations of reactive oxygen mediate their effects, in part via LPO, we measured the levels of LPO in lung homogenates. We observed 3.6- and 2.8-fold increase in the level of LPO in SWCNT and MWCNT exposed mice, respectively, as compared with control (Fig. 8*C*), which directly correlates with increased ROS and MPO levels observed in exposed mice.

Carbon Nanotubes Decrease Antioxidant Level—Antioxidants such as SOD and GSH have been reported in cells involved in protective mechanism during oxidative stress and apoptotic cell death. Because we observed the alteration in the level of ROS, we examined the antioxidant levels in lung homogenates (Fig. 9). A significant decrease in the activity of total SOD was observed in lung homogenates from mice exposed to CNTs as compared with control. Nearly a 40 and 30% reduction of SOD activity was detected in SWCNT- and MWCNT-exposed mice, respectively, than the control group (Fig. 9*B*). Next, we examined the level of catalase in the CNT-exposed group. We observed a 50–60% decrease in the catalase level in both CNT-exposed mice as compared with control (Fig. 9*C*). These data solidify the possible role of the carbon nanotubes in the generation of H_2O_2 in lungs of exposed mice. GSH, the master antioxidant system of the cell, is essential for regulation of cellular events. To study the ability of these nanotubes to deplete GSH, we evaluated the GSH activity in lung homogenates. Our investigation showed a decrease in GSH activity by 50 and 30% with SWCNT- and MWCNT-exposed mice, respectively, as compared with control group (Fig. 9*A*). So both CNTs were able to alter the *in vivo* glutathione level suggesting the ability of

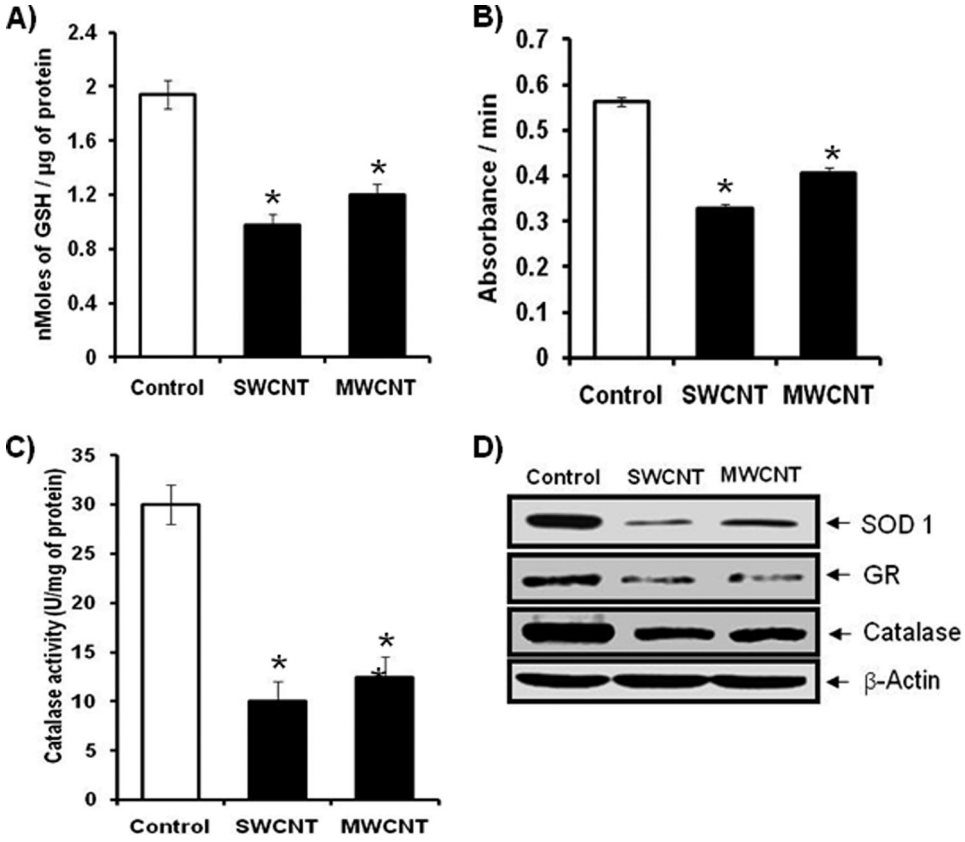

FIGURE 9. **Carbon nanotube inhalation decreases the level of antioxidants in mice.** Proteins were extracted from mice that inhaled CNTs and PBS + 1% Tween 20 (vehicle). *A,* 50 μg of lung homogenates prepared from CNT-exposed and control mouse lungs were used to assay glutathione activity at 415 nm as described under "Experimental Procedures." *B,* 50 μg of proteins was used to assay superoxide dismutase activity using SOD reaction buffer, xanthine, and nitro blue tetrazolium solution according to the manufacturer's instruction. *C,* 50 μg of protein from each sample was mixed with 1 ml of 50 mM potassium phosphate buffer, and catalase activity was measured at 240 nm as described under "Experimental Procedures" for 5 min. Values are means ± S.D. of three experiments performed independently. *, p value <0.05 was estimated by Student's t test. *D,* 50 μg of proteins was resolved on 10% SDS-PAGE and superoxide dismutase (*SOD 1*) and glutathione reductase (*GR*), and catalase was detected using specific antibodies. The blots were stripped off and reprobed with β-actin antibody to ensure equal protein loading.

those particles to reduce antioxidant level in lungs of exposed mice. The decreases in the level of SOD, catalase, and GSH were also confirmed using immunoblot (Fig. 9*D*).

Carbon Nanotubes Induce Caspase-mediated Apoptosis Pathway—Earlier, we reported in the *in vitro* system that MWCNT induces cell death through activation of caspase-3 and -8 (5). Here, we followed the same strategy to verify whether caspase levels are affected by inhalation of CNT in the *in vivo* condition. Analysis of caspase-3, markers of apoptosis, was checked by caspase-3 activity assay and showed significantly increased levels of caspase-3 in the homogenate of mice that inhaled both CNTs (Fig. 10*A*). Caspase-8 activation is dependent on the release of cytochrome *c* from mitochondria to form the apoptosome, which in turn activates caspase-3. Therefore, we also examined the activities of caspase-8 in the same lung homogenates. The assay showed an increased level of caspase-8 in CNT-exposed mice as compared with the controls suggesting the involvement of both forms of CNTs in inducing the apoptotic pathway in BALB/c mice (Fig. 10*B*). Fig 10*C* shows the Western blot analysis for caspase-3 and -8 proteins.

DISCUSSION

The lungs are the most likely route of exposure to air-borne CNTs in addition to the skin. With their morphology similar to asbestos fibers, the assessment of the respiratory toxicity has become a center of attention for many scientists. *In vivo* studies dealing with CNT pulmonary toxicity are currently being conducted to determine the best protocol to be used to study the effect of exposed CNTs. Basically, the airborne particles will interact with its environment through the mechanisms of impaction, sedimentation, and diffusion prior to inhalation, whereas instilled particles in aqueous suspension will not interact (21). The intratracheal instillation or aspiration of SWCNT in rodents causes lung injury (10–12, 20). Moreover, inhaled CNTs are more dispersed and less agglomerated when compared with an instilled bolus dose in aqueous liquid (22). Furthermore, inhalation is much more appropriate than injection of materials into the body cavity, which bypasses the lung and its defense and clearance mechanisms entirely (23). So, to determine the *in vivo* toxicity of CNTs, the inhalation method will be the most relevant and precise. Therefore, the primary objective in this study was to investigate and compare the pulmonary toxicity of occupationally relevant single- and multi-wall carbon nanotube exposures using male BALB/c mice.

We recently reported that the MWCNTs generate ROS and deplete antioxidant levels in exposed rat lung epithelial cells. The exposed cells also showed the activation of NF-κB and

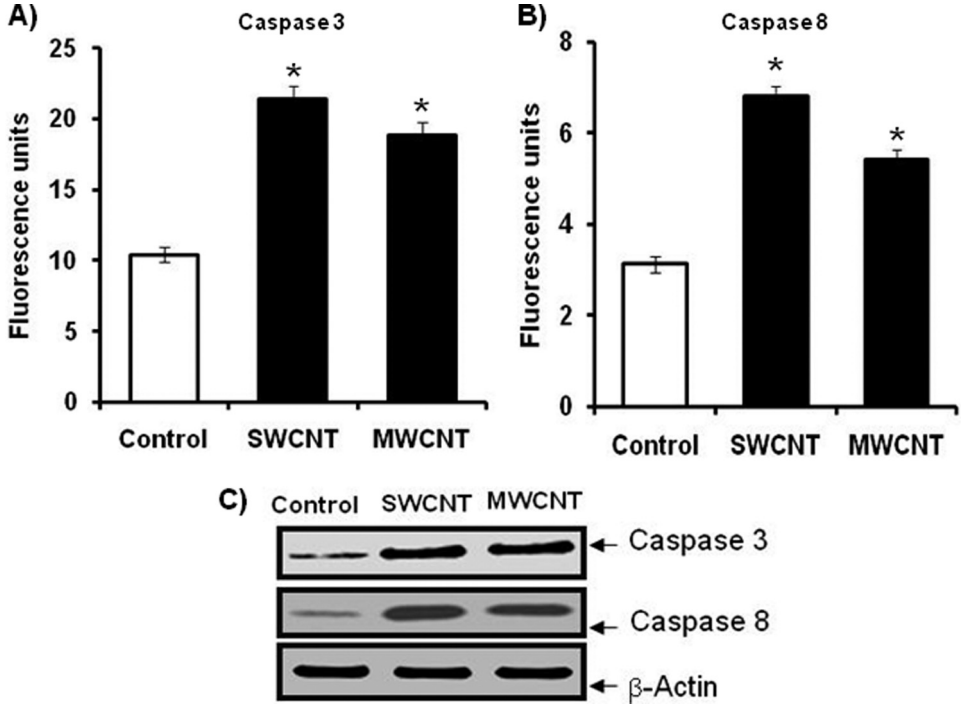

FIGURE 10. **Induction of caspase-3 and -8 activities in carbon nanotube-exposed mice.** 50 μg of protein were extracted from mice that inhaled CNTs and control mouse lungs. *A* and *B,* extracted proteins were mixed with DEVD-AFC and IETD-AFC for caspase-3 and -8 activity, respectively, and the formation of free AFC in the mix was measured at an excitation wavelength of 400 nm and an emission of 495 nm. The experimental values were compared with control and expressed as fluorescence units. Values are means ± S.D. of three independent experiments. *, p value <0.05 was estimated by Student's t test. *C,* Western blot showing caspase-3 and -8 proteins in mice that inhaled CNTs (5 μg/g of mouse) and control mouse lungs. The blots were stripped off and reprobed with β-actin antibody to ensure equal protein loading.

AP-1 signaling pathways to induce apoptotic cell death. In addition, MWCNT activated several death-related proteins, including apoptosis-inducing factor, p53, p21, and Bax in *in vitro* conditions. Therefore, we were interested in checking whether the same effect happens in the *in vivo* condition, particularly the exposed lung tissues. It is important to note that the exposure of CNTs to the cells or animals might vary. Nevertheless, our *in vitro* and *in vivo* data suggest that CNTs have the cytotoxic effects by altering oxidant and antioxidant levels.

To accomplish this, we made the BALB/c mice inhale the aerosol of both types of CNTs in a concentration of ~100 μg/mouse/day for 7 consecutive days in the nose-only exposure system. Recently, a laboratory-based study on air samples during SWCNT mechanical agitation showed a concentration of SWCNT between 0.70 and 53 $\mu g/m^3$; however, more revealing was the concentration present on individual gloves of laboratory workers, which ranged from 217 to 6020 μg (2). To evaluate the relevance of the findings of this *in vivo* mouse study to human CNT exposure, we need to determine whether the doses tested in mice are relevant to human occupational exposures. Assuming a mouse alveolar epithelium surface area of 0.05 m^2 (24), the ~0.6-mg CNT dose would result in an ~12-mg CNT/m^2 alveolar epithelium. A recent study reported that 10 μg of MWCNT exposure in mouse approximates human deposition for a person performing light work for 1 month in a work environment with MWCNT aerosol of 400 $\mu g/m^3$ (25). Even if the average daily CNT aerosol is determined to be much lower, *e.g.* 400 $\mu g/m^3$, it would take approximately 5 years for the 0.6 mg of CNT to deposit in the human lungs. Thus, these estimates suggest that the CNT doses tested in mice in this study approximate reasonable human occupational exposure to SWCNT and MWCNT.

Previous studies have reported that PMNs accumulated in the lungs after inhalation of nanoparticles produce mediators such as cytokines and oxidants, respectively, which is responsible for the fibrotic response (12). Thus, we determined the amplitude and the characteristics of the inflammatory response after inhalation og CNTs. As shown in Fig. 6*A*, significant increases in the total cell numbers in BAL fluid were observed in all treated mice. Also, CNT-induced inflammation was demonstrated by increased levels of LDH and proteins as well as a marked neutrophilic and macrophage accumulation (Fig. 7, *A* and *B*). Thus, it appeared that alveolar macrophages were activated by CNTs and that they attracted immune cells such as neutrophils and monocytes from the bloodstream (Fig. 6, *B* and *C*). The apparently higher degree of inflammation induced by SWCNT compared with MWCNT is possibly the reflection of the better dispersion of these particles in the deep lung, causing greater alveolar cell toxicity and increased alveolocapillar permeability.

Pulmonary fibrosis occurs as a result of increased tissue reactivity leading to the formation and accumulation of fibrous connective tissue. Recently, some researchers have also observed the presence of MWCNTs in the subpleural region in lungs of mice giving rise to fibrosis and scarring (22). In agreement with other reports, here we have observed a significant increased level of collagen in CNT-exposed lung homogenates as compared with control mice (Fig. 5).

Oxidative stress is thought to play an important role in the pathogenesis of various types of lung inflammation, including

allergic asthma (26). Our previous publications on *in vitro* studies showed that CNT toxicity is directly related to an increase in ROS production and is capable of modifying the activity of proteins at the post-translational level and regulating gene expression via important transcriptional factors, which confers an additional inflammatory cascade (6, 7). It had been reported that intratracheally administered SWCNTs exacerbated allergen-related airway inflammation, increased many pro-inflammatory cytokines, and potentiated the formation of oxidative stress (27). Because we observed an increased level of LDH and protein in the BALF of CNT-exposed mouse lungs, we were interested in checking whether CNT exposure induces oxidative stress or not. Similar to earlier findings, we show here a significant increase in the level of MPO and ROS in the BALF/lung homogenates from both CNT-exposed mice compared with controls (Fig. 8, *A* and *B*). In addition, an important biomarker of oxidative stress, induced by reactive free radicals, lipid peroxidation was also induced in CNT-exposed lungs as compared with control (Fig. 8*C*).

To maintain cell integrity, a balance should be maintained between the free radical production and anti-oxidant defense system. Results of this study have shown the significant decreased levels of glutathione, catalase, and SOD activity in exposed mice (Fig. 9, *A–C*), which supports the earlier findings of Oberdörster (28). Nevertheless, SWCNT produced a marked depletion of anti-oxidant levels than did MWCNT, which may be due to the size-dependent induction of oxidative stress by nanoparticles, which supports the earlier results (29).

Caspases are a family of cysteine proteases that play essential roles in apoptosis (30). Here, we have shown the increased levels of caspase-3 and -8 activities, which confirms that inhaled CNTs induce apoptotic pathways in lung tissue (Fig 10, *A* and *B*). Earlier, we have published similar *in vitro* observations in cells exposed to CNTs and proton irradiation (5, 17).

In conclusion, this study shows that inhaled SWCNT and MWCNT induced an inflammatory reaction in lungs activating alveolar macrophages, resulting in the attraction of immune cells to the BAL fluid that results in rapid development of pulmonary fibrosis. Also, we have shown that both inhaled CNTs elevate the oxidative stress and induce lipid peroxidation, which collapsed the antioxidant defense mechanism, and activate the initiator and effector caspases, which may lead to apoptosis in mice following inhalation of carbon nanotubes. This work suggests that careful handling of carbon nanotubes is necessary to minimize the inhalation of nanotubes, until further long term assessments are conducted. Currently, we are investigating the detailed *in vivo* molecular events to assess the degree of damage caused during inhalation of CNTs.

Acknowledgment—We thank Dr. Michael J. Dykstra, North Carolina State University, for technical assistance performing transmission electron microscopy for lung tissues.

REFERENCES

1. Jorio, A., Dresselhaus, G., and Dresselhaus, M. S. (eds) (2008) *Carbon Nanotubes, Topics in Applied Physics,* pp. 13–61, Springer-Verlag, Berlin
2. Maynard, A. D., Baron, P. A., Foley, M., Shvedova, A. A., Kisin, E. R., and Castranova, V. (2004) *J. Toxicol. Environ. Health* **67,** 87–107
3. Fenoglio, I., Tomatis, M., Lison, D., Muller, J., Fonseca, A., Nagy, J. B., and Fubini, B. (2006) *Free Radic. Biol. Med.* **40,** 1227–1233
4. Li, N., Xia, T., and Nel, A. E. (2008) *Free Radic. Biol. Med.* **44,** 1689–1699
5. Ravichandran, P., Periyakaruppan, A., Sadanandan, B., Ramesh, V., Hall, J. C., Jejelowo, O., and Ramesh, G. T. (2009) *J. Biochem. Mol. Toxicol.* **23,** 333–344
6. Manna, S. K., Sarkar, S., Barr, J., Wise, K., Barrera, E. V., Jejelowo, O., Rice-Ficht, A. C., and Ramesh, G. T. (2005) *Nano Lett.* **5,** 1676–1684
7. Ravichandran, P., Baluchamy, S., Sadanandan, B., Gopikrishnan, R., Biradar, S., Ramesh, V., Hall, J. C., and Ramesh, G. T. (2010) *Apoptosis* **15,** 1507–1516
8. Shvedova, A. A., Kisin, E., Murray, A. R., Johnson, V. J., Gorelik, O., Arepalli, S., Hubbs, A. F., Mercer, R. R., Keohavong, P., Sussman, N., Jin, J., Yin, J., Stone, S., Chen, B. T., Deye, G., Maynard, A., Castranova, V., Baron, P. A., and Kagan, V. E. (2008) *Am. J. Physiol. Lung Cell Mol. Physiol.* **295,** L552–L565
9. Huczko, A., Lange, H., Calko, E., Grubek-Jaworska, H., and Droszcz, P. (2001) *Fullerene Sci. Tech.* **2,** 251–254
10. Warheit, D. B., Laurence, B. R., Reed, K. L., Roach, D. H., Reynolds, G. A., and Webb, T. R. (2004) *Toxicol. Sci.* **77,** 117–125
11. Shvedova, A. A., Kisin, E. R., Mercer, R., Murray, A. R., Johnson, V. J., Potapovich, A. I., Tyurina, Y. Y., Gorelik, O., Arepalli, S., Schwegler-Berry, D., Hubbs, A. F., Antonini, J., Evans, D. E., Ku, B. K., Ramsey, D., Maynard, A., Kagan, V. E., Castranova, V., and Baron, P. (2005) *Am. J. Physiol. Lung Cell Mol. Physiol.* **289,** L698–L708
12. Muller, J., Huaux, F., Moreau, N., Misson, P., Heilier, J. F., Delos, M., Arras, M., Fonseca, A., Nagy, J. B., and Lison, D. (2005) *Toxicol. Appl. Pharmacol.* **207,** 221–231
13. Cho, W. S., Choi, M., Han, B. S., Cho, M., Oh, J., Park, K., Kim, S. J., Kim, S. H., and Jeong, J. (2007) *Toxicol. Lett.* **175,** 24–33
14. Sharma, C. S., Sarkar, S., Periyakaruppan, A., Barr, J., Wise, K., Thomas, R., Wilson, B. L., and Ramesh, G. T. (2007) *J. Nanosci. Nanotechnol.* **7,** 2466–2472
15. Periyakaruppan, A., Kumar, F., Sarkar, S., Sharma, C. S., and Ramesh, G. T. (2007) *Arch. Toxicol.* **81,** 389–395
16. Haegens, A., van der Vliet, A., Butnor, K. J., Heintz, N., Taatjes, D., Hemenway, D., Vacek, P., Freeman, B. A., Hazen, S. L., Brennan, M. L., and Mossman, B. T. (2005) *Cancer Res.* **65,** 9670–9677
17. Baluchamy, S., Ravichandran, P., Periyakaruppan, A., Ramesh, V., Hall, J. C., Zhang, Y., Jejelowo, O., Gridley, D. S., Wu, H., and Ramesh, G. T. (2010) *J. Biol. Chem.* **285,** 24769–24774
18. Aebi, H. (1984) *Methods Enzymol.* **105,** 121–126
19. Fahmy, B., Ding, L., You, D., Lomnicki, S., Dellinger, B., and Cormier, S. A. (2010) *Environ. Toxicol. Pharmacol.* **29,** 173–182
20. Lam, C. W., James, J. T., McCluskey, R., and Hunter, R. L. (2004) *Toxicol. Sci.* **77,** 126–134
21. Miller, F. J. (2000) *Inhal. Toxicol.* **12,** 19–57
22. Ryman-Rasmussen, J. P., Tewksbury, E. W., Moss, O. R., Cesta, M. F., Wong, B. A., and Bonner, J. C. (2009) *Am. J. Respir. Cell Mol. Biol.* **40,** 349–358
23. Poland, C. A. Duffin, R., Kinloch, I., Maynard, A., Wallace, W. A., Seaton, A., Stone, V., Brown, S., MacNee, W., and Donaldson, K. (2008) *Nat. Nanotech.* **3,** 423–428
24. Stone, K. C., Mercer, R. R., Gehr, P., Stockstill, B., and Crapo, J. D. (1992) *Am. J. Respir. Cell Mol. Biol.* **6,** 235–243
25. Porter, D. W., Wolfarth, M. G., Chen, B. T., McKinney, W., Hubbs, A. F., Battelli, L., Andrew, A., Frazier, D. G., and Castranova, V. (2009) *Toxicologist* **108,** 457
26. Riedl, M. A., and Nel, A. E. (2008) *Curr. Opin. Allergy Clin. Immunol.* **8,** 49–56
27. Inoue, K., Yanagisawa, R., Koike, E., Nishikawa, M., and Takano, H. (2010) *Free Radic. Biol. Med.* **48,** 924–934
28. Oberdörster, E. (2004) *Environ. Health Perspect.* **112,** 1058–1062
29. Wang, F., Gao, F., Lan, M., Yuan, H., Huang, Y., and Liu, J. (2009) *Toxicology In Vitro* **23,** 808–815
30. Shi, Y. G. (2002) *Mol. Cell* **9,** 459–470

Pulmonary Biocompatibility Assessment of Inhaled Single-wall and Multiwall Carbon Nanotubes in BALB/c Mice

Prabakaran Ravichandran, Sudhakar Baluchamy, Ramya Gopikrishnan, Santhoshkumar Biradar, Vani Ramesh, Virupaxi Goornavar, Renard Thomas, Bobby L. Wilson, Robert Jeffers, Joseph C. Hall and Govindarajan T. Ramesh

J. Biol. Chem. 2011, 286:29725-29733.
doi: 10.1074/jbc.M111.251884 originally published online June 24, 2011
